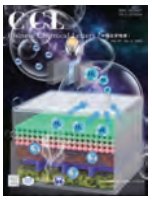
Chinese Chemical Letters 37 (2026) 111086

Contents lists available at ScienceDirect

Chinese Chemical Letters

journal homepage: www.elsevier.com/locate/cclet



Zinc coordination self-assembly of bacitracin nanoparticles with broadened antibacterial spectrum

Jiaye Wang[a,b,1], Xiong Yang[a,b,1], Yang Lei[a,b], Tianwen Xi[a,b], Sijie Wang[a], Yidan Zhou[a], Bing Liu[c,*], Yu Liu[d,*], Hui Yang[a,*], Leming Sun[a,b,*]

[a] School of Life Sciences, Engineering Research Center of Chinese Ministry of Education for Biological Diagnosis, Treatment and Protection Technology and Equipment in Special Environment, Northwestern Polytechnical University, Xi'an 710072, China
[b] Dongguan Sanhang Innovation Institute, Dongguan 523808, China
[c] College of Life and Environmental Science, Wenzhou University, Wenzhou 325035, China
[d] Department of Cardiology, Nanjing University Medical School Affiliated Nanjing Drum Tower Hospital, Nanjing 210008, China

ARTICLE INFO

Article history:
Received 16 July 2024
Revised 9 March 2025
Accepted 12 March 2025
Available online 12 March 2025

Keywords:
Self-assembly
Bacitracin
Nanoparticle
Antibacterial
Membrane penetration

ABSTRACT

Bacitracin has been extensively studied for its antibacterial application due to its excellent anti-Gram-positive bacterial properties. However, its application of conventional bacitracin has been limited because of its limited antibacterial activity against Gram-negative bacteria, especially negative bacilli. In this study, we designed and synthesized bacitracin-zinc nanodrugs (BPNDs) through zinc coordination self-assembly of bacitracin, which exhibit potent antibacterial effects not only against Gram-positive bacterial *Staphylococcus aureus* but also against *Escherichia coli*, a typical Gram-negative bacillus. The morphological and antimicrobial properties of the self-assembled BPNDs with different molar ratios of bacitracin to zinc ions were investigated. The bacterial biofilm experiments confirmed the biofilm scavenging effect of BPNDs, further expanding the application of this antimicrobial agent. In-depth cell viability experiments indicated that this antimicrobial activity might be related to the penetration of BPNDs into bacterial cell membranes. This study reveals that the zinc-coordinated peptide self-assembly strategy expands the antibacterial spectrum of conventional bacitracin, making it a potential candidate for novel antimicrobial drugs to address the bacterial resistance dilemma and provide stable alternatives for a wide range of biomedical and related industries.

© 2026 Published by Elsevier B.V. on behalf of Chinese Chemical Society and Institute of Materia Medica, Chinese Academy of Medical Sciences.

Bacitracin, also known as bacillus peptide, is a broad-spectrum cyclic peptide antibiotic complex produced mainly by *Bacillus subtilis* and *Bacillus licheniformis*, which also can be synthesized by non-ribosomal peptide synthetase (NRPS). Bacitracin has a good killing effect on most Gram-positive bacteria, especially bacilli and cocci [1–3]. Bacitracin has been proven to inhibit the synthesis of the bacterial cell wall and galactosidase. Moreover, bacitracin can disrupt the permeability of the cell membrane to prevent bacterial proliferation. In general, bacitracin has excellent properties such as a wider antibacterial spectrum, low residual rate, and low tendency to induce drug resistance, so it can be used as ideal materials for designing potent peptide-based antibiotics, and they are the pioneering drugs for rational design of peptide antibiotics in the future [4–6].

Bacitracin is composed of 11 amino acids (Cys, L-Leu, D-Glu, L-Ile, L-Lys, D-Orn, L-Val, D-Phe, L-His, D-Asp, L-Asn) as its precursor [7]. There are several classes of bacitracin, including bacitracin A, bacitracin B (including B1, B2, and B3), bacitracin C (including C1, C2, and C3), and bacitracin F. The various bacitracin peptides have minor differences in amino acids composition. Among these bacitracins, bacitracin A has the highest biological activity [8,9], which has been widely utilized in the livestock and pharmaceutical industries, where little resistance has been reported [10–12]. Bacitracin A binds to undecaprenyl pyrophosphate and targets its site of action, preventing the recycling of sugar carriers and inhibiting bacterial cell wall synthesis. Bacitracin A can also dissociate the bacterial cytoplasmic membrane, causing loss of amino acids and various ions, and ultimately bacterial death. However, because of its complex chemical structure and high molecular weight, bacitracin A cannot pass through the porin proteins in the outer membrane of Gram-negative bacteria to reach the cell wall at its site of action [13].

* Corresponding authors.
E-mail addresses: hkliubing6698@wzu.edu.cn (B. Liu), lycqx@aliyun.com (Y. Liu), kittyyh@nwpu.edu.cn (H. Yang), lmsun@nwpu.edu.cn (L. Sun).
[1] These authors contributed equally to this work.

https://doi.org/10.1016/j.cclet.2025.111086
1001-8417/© 2026 Published by Elsevier B.V. on behalf of Chinese Chemical Society and Institute of Materia Medica, Chinese Academy of Medical Sciences.

Nanodrug delivery systems (NDDs) have emerged as a rapidly evolving field, enabling the diagnosis and effective treatment of diseases such as inflammation, cancer, neurological disorders, and cardiovascular diseases [14–17]. Encapsulating or combining antibiotics in nanocarriers can effectively improve the interaction between antibiotics and pathogenic microorganisms, so the use of nanoparticles as carriers for antimicrobial drug delivery could be a strategy to solve the above problem [18]. Peptide self-assembled materials have attracted wide interest in biomedical applications due to their biocompatibility and biodegradability [19–21]. Based on non-covalent interactions between molecules, such as hydrogen bonding, π-π stacking, electrostatic interactions, hydrophobic and van der Waals interactions, peptides can be self-assembled into a variety of nanostructures such as nanoparticles, nanotubes, nanoribbons, and nanofibers [22–28]. In contrast to conventional peptide self-assembly strategies that involve complex modifications on peptides, we have developed a general peptide self-assembly strategy regulated by metal ion coordination [20,29–31]. In this study, bacitracin and zinc ions were successfully assembled into a novel bacitracin nanodrug using the peptide self-assembly technique, and morphological characterization and antimicrobial activity were performed. The bacillus peptide-zinc ion nanodrugs (BPNDs) exhibited higher stability and showed a significant killing effect against the Gram-positive bacterium *Staphylococcus aureus* (*S. aureus*) and Gram-negative bacterium *Escherichia coli* (*E. coli*). Moreover, it showed significant disruptive and inhibitory effects on Gram-negative bacterial cell membranes in the biofilm test, which overcame the application limitation that bacitracin A monomers could not kill Gram-negative bacteria and broadened the antibacterial spectrum of bacitracin A monomers. In addition, the unique nature of nanodrugs enables them to reduce side effects and increase the effective drug delivery rate by improving the pharmacokinetics and target accumulation of antibiotics [32–34].

The experimental steps are described in Supporting information. We developed and utilized a general peptide self-assembly strategy regulated by metal ion coordination to assemble bacitracin A and zinc ions into a series of novel bacitracin nanodrugs BPNDs (Fig. 1). The effect of bacitracin A to Zn(II) ratios on the self-assembly of BPNDs was investigated with varying molar ratios (2:1, 1:1 and 1:10). The BPNDs synthesized with the above three reaction systems were abbreviated as BPNDs-1, BPNDs-2, and BPNDs-3. Based on these results, experiments were conducted to test the bacteriostatic properties of the synthesized BPNDs at different bacitracin substrate concentrations (1 and 5 mg/mL). The results of the zone of inhibition experiments showed that the BPNDs synthesized with 1 mg/mL bacitracin A solution as the substrate had a higher stability of bacterial inhibition under the same conditions (Fig. S1 in Supporting information). This stability advantage was evident

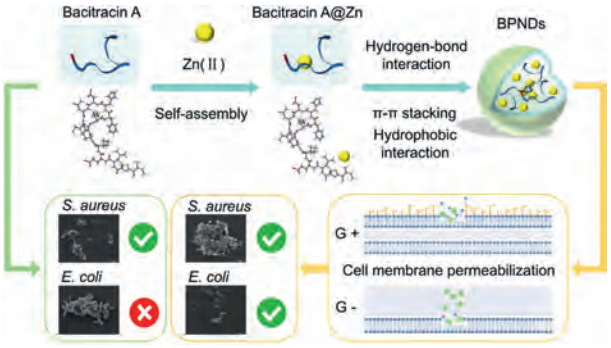


Fig. 1. Bacitracin A and zinc ions self-assemble to form BPNDs by hydrothermal synthesis under the combined effects of hydrogen bonding, π-π stacking, and zinc coordination. Unlike conventional bacitracin, BPNDs exerts its antimicrobial effect on Gram-negative bacillus through membrane permeabilization.

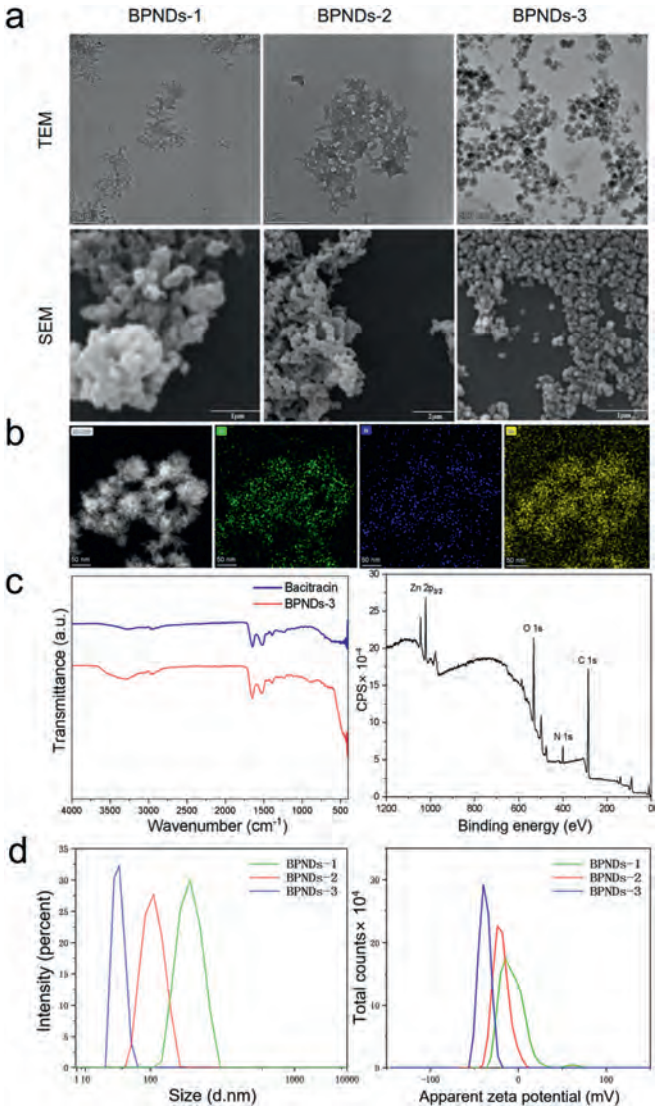


Fig. 2. Material characterization of BPNDs. (a) Transmission and scanning electron microscopy analysis of BPNDs synthesized at different bacitracin A to zinc molar ratios. (b) Energy spectroscopy profiles of BPNDs-3. (c) FTIR spectra of BPNDs-3 and bacitracin A and XPS analysis spectrum of BPNDs-3. (d) DLS analysis of particle size and zeta potential for three types of BPNDs.

for all BPNDs synthesized at different molar ratios and all of them showed significant bacteriostatic activity, which facilitates subsequent discussion and study.

After the preliminary experiments, the morphological features of the BPNDs were investigated at different molar ratios. The synthesized BPNDs were characterized using transmission electron microscopy (TEM). As shown in Fig. 2a, BPNDs-1 and BPNDs-2 exhibited similar lamellar agglomerates with sizes ranging from 500 nm to 1000 nm. BPNDs-1 and BPNDs-2 are tightly aggregated under TEM imaging to form a lamellar stacking prototype, with tight network laminar structures appearing in the lamellar facet breaks. In contrast, BPNDs-3 was a nanodendritic cluster structure with a diameter around 50–100 nm, as shown in Fig. 2b. This self-assembled nanostructure was more regular and uniformly distributed, which improved the homogeneity of the nanodrugs.

The morphology of the nanoparticles was also characterized with the aid of scanning electron microscopy (SEM). The experimental results of TEM and SEM images corresponded as expected in Fig. 2a. The BPNDs prepared from the precipitated suspensions of the experimental groups at ratios of 2:1 and 1:1 was tightly

and heavily aggregated. This may be because the bacitracin A monomers can form a laminar accumulation after chelating a certain amount of zinc ions during the heating process. A compact "vesicle-like laminar" structure was observed at the fracture of the laminar surface. In the 1:10 molar ratio of the experimental group, the precipitated suspensions of bacitracin nanoparticles showed a snowflake-like flake distribution, and this snowflake-like structure was the large nanoparticles, which were also formed by the aggregation of a very large number of small nanoparticles. This result also proved that the synthesized regular nanoparticles can be the next direction for experimentation and exploration. The experimentally synthesized BPNDs-3 was analyzed by energy spectroscopy and nitrogen, oxygen and zinc were uniformly distributed along the synthesized nanoparticle imprints, which is in accordance with the experimental expectations in Fig. 2b. The presence of nitrogen atoms in the energy spectrum analysis proved the successful synthesis of self-assembled nanoparticles with zinc and peptides. The synthesized BPNDs-3 was analyzed by X-ray diffraction (XRD) and it was found to have characteristic diffraction peaks, identifying the synthesized product as a crystalline form (Fig. S2 in Supporting information). The Fourier transform infrared spectroscopy (FTIR) spectra of BPNDs-3 and bacitracin are compared and the result showed that a new metal-oxygen stretching band at 430 cm^{-1}, assigned to a characteristic absorption peak of zinc oxide, as compared to the amino acids alone (Fig. 2c). FTIR also showed that the peaks of BPNDs and monomers were basically the same except for the difference mentioned above, proving that there was no change in the structure of the nanodrug. In addition, X-ray photoelectron spectroscopy (XPS) measurements confirmed the presence of zinc along with carbon (C), nitrogen (N) and oxygen (O) atoms. The dynamic light scattering (DLS) test results in Fig. 2d showed that BPNDs-3 demonstrated higher stability compared to the other two materials, with a smaller particle size and a more uniform distribution.

To study the underlying mechanism, we investigated the bacteriostatic efficacy of zinc oxide nanoparticles (control), bacitracin A monomer, and the self-assembled BPNDs-3 by agar well diffusion assay using *S. aureus* (Fig. 3a). Bacitracin A and BPNDs-3 were found to have good bacteriostatic properties against *S. aureus* at concentrations of 0.05, 0.275 and 0.5 mg/mL, but control groups showed no obvious antibacterial effects. The inhibitory effect of the synthesized BPNDs-3 was compared with that of monomeric mycopeptides by measuring the area of the inhibition zone treated under the same conditions. It could be found that the synthesized BPNDs-3 possessed better bacterial inhibition under the same conditions.

After zone of inhibition test, the co-incubation method was taken to explore the bacteriostatic effect of BPNDs against *S. aureus* and *E. coli*. Synchronized treated diluted suspensions of *S. aureus* and *E. coli* and equal volumes of different samples (suspensions) including control, BPNDs-1, BPNDs-2, and BPNDs-3 were made up to 1 mL of the reaction system, which was replenished with 10 mmol/L sterile phosphate buffered saline (PBS). After co-incubation for 5–6 h, it was spread evenly on agar plates. After co-incubation of *S. aureus* with the different groups, the results of the inhibition experiments were observed in Fig. 3b, Fig. S3 and Table S1 (Supporting information). The control group treated with aqueous bacitracin A monomer solution at room temperature showed the highest number of colonies, indicating that the aqueous bacitracin A monomer solution loses its ideal antimicrobial properties due to biological degradation based on several factors such as temperature and time. Observing the experimental group of plates, all the three molar ratios of synthesized BPNDs exhibited good bacterial inhibition. From BPNDs-1, BPNDs-2 to BPNDs-3, the number of *S. aureus* colonies was reduced and the inhibitory effect became more and more significant. Most importantly, the growth

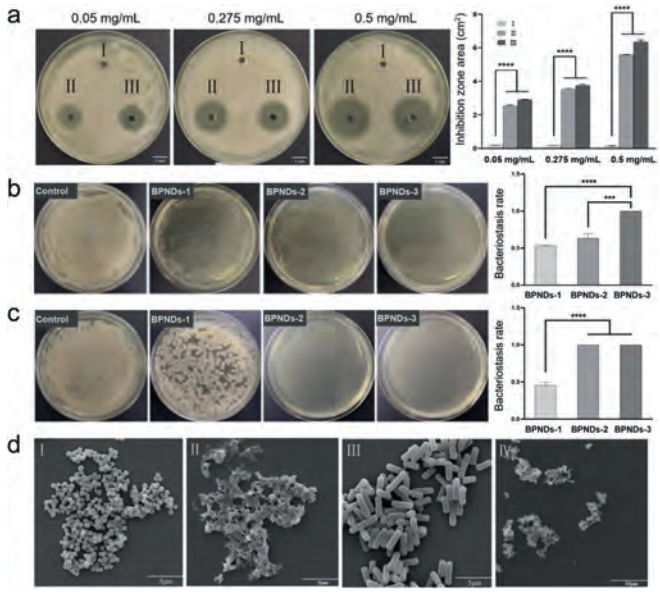


Fig. 3. Characterization of the antibacterial properties of BPNDs. (a) Antimicrobial (*S. aureus*) properties characterization of bacitracin monomer and BPNDs-3. I: Control (zinc oxide nanoparticles solution). II: Monomeric bacitracin solution. III: BPNDs-3. The data was analyzed and collated in bar charts. Scale bar: 1 cm. (b) Characterization of the antibacterial properties of BPNDs against *S. aureus*. Relative inhibition rates were analyzed and collated in bar charts. (c) Characterization of the antibacterial properties of BPNDs against *E. coli*. Relative inhibition rates were analyzed and collated in bar charts. (d) SEM analysis before and after BPNDs-3 treatment. I: *S. aureus* before treatment. II: *S. aureus* after treatment. III: *E. coli* before treatment. IV: *E. coli* after treatment. Scale bar: 5 μm (I, II, III), 10 μm (IV). $^{***}P < 0.001$, $^{****}P < 0.0001$. Data are presented as mean ± standard deviation (SD) ($n = 5$).

of colonies was not seen at all in the co-incubated syntheses of BPNDs-3 experimental group. SEM analysis in Fig. 3d II showed that *S. aureus* basically lost its normal morphology after BPNDs-3 treatment, which aided in verifying the good bacteriostatic properties of BPNDs against Gram-positive bacteria. After co-incubation of *E. coli* with the treated group, the results of the inhibition experiments were observed in Fig. 3c, Fig. S4 and Table S2 (Supporting information). The control group of aqueous solution of bacitracin A monomer treated at room temperature showed the highest number of colonies, proving the instability of bacitracin A monomer. For the experimental group, it was observed that the bacteriostatic effect of BPNDs became more and more significant from BPNDs-1, BPNDs-2 to BPNDs-3. SEM analysis in Fig. 3d IV showed that *E. coli* basically lost the original morphology of bacteria after BPNDs-3 treatment, which verified the good bacteriostatic effect of BPNDs on *E. coli*. Bacitracin A has a complex chemical structure and high molecular weight, and cannot cross the pore proteins in the outer membrane of Gram-negative bacteria to reach the cell wall region of its action site. However, no colony growth was observed in BPNDs-treated *E. coli* experimental plates after co-incubation with the complex at a ratio of 1:1, which proved its killing effect on Gram-negative bacteria and overcame the limitation of the application of monomer bacitracin A that could not kill the negative bacteria.

The effect of BPNDs on biofilm was characterized to investigate the anti-biofilm properties. Bacterial biofilm (BF) is a structure attached to the surface of inanimate or living organisms during the growth process of bacteria, and is formed by bacteria and their secreted extracellular polymers. Before performing the experiments, we determined the minimum inhibitory concentration (MIC) of BPNDs-3 against *S. aureus* and *E. coli*, respectively. The MIC was defined as the minimum concentration at which there

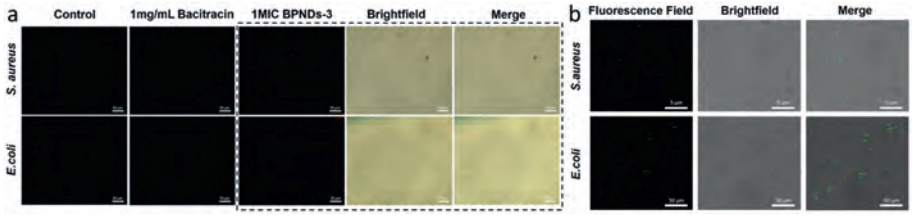


Fig. 4. (a) Changes in cell viability after treatment of *S. aureus* and *E. coli* with the synthesized BPNDs-3 were analyzed by fluorescence microscopy respectively. Scale bar: 50 μm. (b) Tracking and characterization of fluorescently labeled nanodrugs. Scale bar: 5 μm (*S. aureus* groups), 50 μm (*E. coli* groups).

was no growth of bacterial species after 18 h of incubation. The MIC value of BPNDs-3 against *E. coli* was 909 μg/mL, while the MIC value against *S. aureus* was 56.8 μg/mL. Afterward, the clearance of BPNDs-3 was evaluated in the biofilm by crystal violet (CV) staining and the experimental data were plotted in Table S3 (Supporting information). After 3 h of co-incubation treatment of BPNDs-3 with biofilm, the biofilm removal effect on *E. coli* and *S. aureus* was satisfactory, and the biofilm removal rate in the 1 MIC treatment group reached >20 %, and the incremental increase of the removal rate with the increase of the concentration of the BPNDs-3 was more obvious, which was consistent with the expected results.

An exploration of the antimicrobial mechanism of BPNDs-3 was carried out by assessing cell viability by fluorescent staining (Fig. 4a). After co-incubation of different concentrations of BPNDs-3 and appropriate concentrations of two bacterial dilutions for 2 h, the cells were stained using propidium iodide and observed under a fluorescence microscope. Observation by fluorescence microscopy revealed that under the above experimental conditions, the 0.5 and 1 MIC groups showed remarkable red fluorescence, and the fluorescence density increased incrementally with the increase of BPNDs-3 concentration, indicating significant cell death (Fig. 4 and Fig. S5 in Supporting information). In addition, it was observed that the bacitracin monomer-treated group did not show significant red fluorescence, and it was suggested that the bacteriostatic ability of the bacitracin monomer was inhibited or completely disappeared during the treatment. Under the same treatment conditions, bacitracin monomer was unable to exert a significant bacteriostatic effect on *E. coli*. It was inferred that the presence of BPNDs-3 increased the permeability of the cell membrane, allowing the fluorescent dye to enter the cell and bind to DNA. In addition, the PI static fluorescence of the samples was measured by fluorescence spectrophotometer (Figs. S6 and S7 in Supporting information). It was found that static fluorescence increased with increasing drug concentration in both *E. coli* and *S. aureus* treatment groups. There were only minor differences in the static fluorescence of the treatment groups at different times, proving that the drug exerted most of its effects within 30 min.

The redox method was also used to investigate the effect of BPNDs-3 on bacterial metabolic levels (Table S4 in Supporting information). The results showed that the nanodrug BPNDs-3 had a greater impact on the metabolism of bacteria, including *E. coli* and *S. aureus*, compared to the traditional antibiotic bacitracin. This suggests that BPNDs-3 may exert its antibacterial activity, at least in part, by influencing bacterial metabolism. By labeling BPNDs-3 with green fluorescent protein, we observed and tracked the binding of the nanodrug to bacteria (Fig. 4b). It was found that BPNDs-3 accumulated extensively within *S. aureus*, while only a small amount of the drug was present inside *E. coli*, with most of the drug surrounding the *E. coli* cells. This experimental observation reveals that BPNDs-3 exhibits high affinity and uptake capacity for *S. aureus*, but a weaker effect on *E. coli*. This suggests that BPNDs-3 may have a targeted action or stronger cell membrane penetration ability against *S. aureus*, while its interaction with *E. coli* is less pronounced. This difference may be attributed to the natural structural variations between *S. aureus* and *E. coli*. However, it is undeniable that BPNDs-3 demonstrates bactericidal activity against *E. coli*, overcoming the limitations of traditional Bacitracin. It is speculated that the bactericidal effect on *E. coli* may occur through mechanisms not only by membrane disruption, but other ways such as affecting its metabolic pathways.

In summary, we report a bacitracin nanodrug synthesized by zinc coordination, hydrogen bonding and π-π stacking using a novel self-assembly approach. The antimicrobial studies demonstrated that BPNDs could overcome the limitations of the antibacterial spectrum of monomeric bacitracin and showed antibacterial activity against *S. aureus* and *E. coli*. The cell viability assay results revealed that BPNDs could permeabilize the cell membranes of the bacteria, leading to damage to the cell membranes, and thus inducing cell death. Therefore, zinc coordination peptide self-assembly may be a novel way to broaden the antimicrobial spectrum of traditional antimicrobial peptides, which may help to break the current stalemate of increasing bacterial drug resistance. At present, we have only found the feasibility of this approach in bacitracin, and we are very excited about the possibility of applying this method of expanding the antimicrobial spectrum to more traditional drugs.

Declaration of competing interest

The authors declare that they have no known competing financial interests or personal relationships that could have appeared to influence the work reported in this paper.

CRediT authorship contribution statement

Jiaye Wang: Writing – original draft, Methodology, Data curation, Investigation. **Xiong Yang:** Writing – original draft, Methodology, Data curation, Investigation. **Yang Lei:** Methodology, Data curation. **Tianwen Xi:** Methodology, Data curation. **Sijie Wang:** Methodology, Data curation. **Yidan Zhou:** Methodology, Data curation. **Bing Liu:** Writing – review & editing, Validation, Supervision. **Yu Liu:** Supervision, Resources, Project administration. **Hui Yang:** Writing – review & editing, Supervision, Resources, Project administration, Conceptualization. **Leming Sun:** Writing – review & editing, Writing – original draft, Validation, Project administration, Methodology, Investigation, Funding acquisition, Conceptualization.

Acknowledgments

This work was supported by the National Natural Science Foundation of China (No. 31900984), the Natural Science Basic Research Plan in Shaanxi Province of China (No. 2024JC-YBMS-110), the Guangdong Basic and Applied Basic Research Foundation (No. 2022A1515140031), the Fundamental Research Funds for the Central Universities (No. D5000230059), and National Undergraduate Training Programs for Innovation and Entrepreneurship (No. XN2022273).

Supplementary materials

Supplementary material associated with this article can be found, in the online version, at doi:10.1016/j.cclet.2025.111086.

References

[1] Y. Tao, S. Xie, Y. Zhu, et al., J. Chromatogr. Sci. 56 (2018) 285–291.
[2] S. Kyriakis, A. Tsinas, S. Lekkas, et al., Vet. Rec. 138 (1996) 489–492.
[3] R. Engberg, M. Hedemann, T. Leser, et al., Poult. Sci. 79 (2000) 1311–1319.
[4] R. Hancock, Lancet Infect. Dis. 5 (2000) 209–218.
[5] E. Wan, C. Ho, D. Sin, Y. Wong, et al., Anal. Bioanal. Chem. 385 (2006) 181–188.
[6] D. Abbanat, M. Macielag, K. Bush, Anal. Bioanal. Chem. 12 (2003) 379–399.
[7] F. Drabløs, D. Nicholson, M. Rønning, Biochim. Biophys. Acta 1431 (1999) 433–442.
[8] A. Potts, T. Psurek, C. Jones, et al., J. Pharm. Biomed. Anal. 70 (2012) 619–623.
[9] S. Suleiman, F. Song, M. Su, et al., J. Pharm. Anal. 7 (2017) 48–55.
[10] L. Ming, J. Epperson, J. Inorg. Biochem. 91 (2002) 46–58.
[11] C. Sharma, M. Sharma, Mini-Rev. Med. Chem. 17 (2017) 1548–1556.
[12] B. Wagner, D. Schumann, U. Linne, et al., J. Am. Chem. Soc. 128 (2006) 10513–10520.
[13] W. Hong, Y. Zhao, Y. Guo, et al., ACS Appl. Mater. Inter. 11 (2019) 7635.
[14] L. Ou, S. Zhong, J.S. Ou, J.W. Tian, Acta. Pharmacol. Sin. 42 (2012) 10–17.
[15] A. Zia, Y. Wu, T. Nguyen, et al., Cardiovasc. Res. 116 (2020) 2055–2068.
[16] C. Feng, P. Tan, G. Nie, et al., Exploration 3 (2023) 20210263.
[17] Y. Zhang, H. Yang, D. Wei, et al., Exploration 1 (2021) 20210115.
[18] Y. Liu, H. Busscher, B. Zhao, et al., ACS Nano 10 (2016) 4779–4789.
[19] Y. Chen, A. Orr, K. Tao, et al., ACS Nano 14 (2020) 2798–2807.
[20] Y. Wang, Y. Lei, J. Wang, et al., Chin. Chem. Lett. 34 (2023) 107915.
[21] L. Sun, D. Liu, D. Fu, et al., Chem. Eng. J. 405 (2021) 126733.
[22] N. Habibi, N. Kamaly, A. Memic, et al., Nano Today 11 (2016) 41–60.
[23] D. Fu, D. Liu, L. Zhang, et al., Chin. Chem. Lett. 31 (2020) 3195–3199.
[24] L. Sun, A. Li, Y. Hu, et al., Part. Part. Syst. Charact. 36 (2019) 1800420.
[25] L. Sun, Z. Fan, T. Yue, et al., Bio-des. Manuf. 1 (2018) 182–194.
[26] Y. Zhu, X. Deng, Y. Wu, et al., Chin. Chem. Lett. 36 (2025) 109733.
[27] Y. Zhou, W. Zhang, R. Fu, et al., Chin. Chem. Lett. 36 (2025) 109865.
[28] C. Yu, P. Shang, H. Hu, et al., Chin. Chem. Lett. 35 (2024) 109805.
[29] W. Lin, Y. Yang, Y. Lei, et al., ACS Appl. Mater. Inter. 13 (2021) 32799–32809.
[30] Y. Lei, Y. Wang, D. Liu, et al., Chin. Chem. Lett. 33 (2022) 1946–1950.
[31] Z. Fan, L. Sun, Y. Huang, et al., Nat. Nanotechnol. 11 (2016) 388–394.
[32] W. Hong, X. Gao, P. Qiu, et al., Int. J. Nanomed. 14 (2019) 771.
[33] J. Xuan, W. Feng, J. Wang, et al., Drug Resist. Updat. 68 (2023) 100954.
[34] L. Sun, H. Liu, Y. Ye, et al., Signal Transduct. Target. Ther. 8 (2023) 418.